An Unorthodox Reaction of Indene with $ReH_7(PPh_3)_2$: The Competitive Formation of an η^5-Indanyl Ligand versus an η^5-Indenyl Ligand

Glen P. Rosini and William D. Jones*

Contribution from the Department of Chemistry, University of Rochester, Rochester, New York 14627. *Received April 20, 1992*

Abstract: The reaction of indene with $ReH_7(PPh_3)_2$ yields a mixture of two organometallic complexes, identified as (η^5-C_9H_7)$ReH_2(PPh_3)_2$ (**1**) and (η^5-C_9H_{11})$ReH_2(PPh_3)_2$ (**2**). In **1**, the minor (expected) product, the metal is η^5-bound to the five-membered ring, while in **2**, the major product, the metal is η^5-bound to the six-membered ring. When the reaction is run in the presence of 3,3-dimethyl-1-butene, only **1** is formed, while **2** can be obtained pure if the reaction is run under an atmosphere of hydrogen. The mechanism for the formation of **1** and **2** is discussed, as are the photochemical and thermal reactivities of **2**, leading to the formation of (η^6-C_9H_{10})$ReH_3(PPh_3)$ (**5**) and (η^6-C_9H_{10})$ReH(PPh_3)_2$ (**6**), respectively. When bicyclo[4.3.0]nona-3,6(1)-diene is used in place of indene, the product is the unexpected 2,4-diene complex (η^4-C_9H_{12})$ReH_3(PPh_3)_2$ (**7**), which rearranges upon heating to a 1:1.5 mixture of **2** and a complex analogous to **1** with an η^5-bound 4,5,6,7-tetrahydroindene ligand (η^5-C_9H_{11})$ReH_2(PPh_3)_2$ (**8**). Oxidation/protonation of complex **2** results in the formation of complex **9** or **10**, [(η^6-C_9H_{10})$ReH_2(PPh_3)_2$][X] (X = ReO_4, **9**; BF_4, **10**). Complex **1** crystallizes in the triclinic space group $P\bar{1}$ with a = 9.876 (7) Å, b = 14.137 (4) Å, c = 14.375 (12) Å, α = 96.12 (6)°, β = 109.07 (6)°, γ = 107.99 (5)°, V = 1755 (2) Å^3, and Z = 2. Complex **2** crystallizes in the triclinic space group $P\bar{1}$ with a = 10.140 (4) Å, b = 13.993 (5) Å, c = 14.564 (9) Å, α = 95.51 (4)°, β = 109.73 (4)°, γ = 107.58 (3)°, V = 1809 (4) Å^3, and Z = 2. Complex **5** crystallizes in the triclinic space group $P\bar{1}$ with a = 8.626 (3) Å, b = 9.201 (2) Å, c = 16.002 (5) Å, α = 97.43 (2)°, β = 98.34 (3)°, γ = 114.12 (3)°, V = 1122 (1) Å^3, and Z = 2. Complex **6** crystallizes in the monoclinic space group $P2_1/n$ with a = 10.428 (3) Å, b = 17.054 (3) Å, c = 20.100 (4) Å, β = 98.78 (2)°, V = 3532 (1) Å^3, and Z = 4. Complex **7** crystallizes in the monoclinic space group $P2_1/n$ with a = 14.418 (2) Å, b = 16.823 (4) Å, c = 15.838 (7) Å, β = 102.72 (2)°, V = 3747 (3) Å^3, and Z = 4. Complex **8** crystallizes in the triclinic space group $P\bar{1}$ with a = 10.104 (3) Å, b = 14.344 (5) Å, c = 14.475 (5) Å, α = 71.85 (3)°, β = 69.42 (2)°, γ = 71.01 (2)°, V = 1811 (1) Å^3, and Z = 2. Complex **9** crystallizes in the monoclinic space group $P2_1/n$ with a = 11.950 (3) Å, b = 18.836 (8) Å, c = 17.781 (5) Å, β = 98.28 (2)°, V = 3961 (4) Å^3, and Z = 4.

Introduction

The chemistry of transition metal polyhydride complexes has been an area of extensive research for almost three decades now. It has been shown that polyhydride complexes are able to activate both aromatic and aliphatic C–H bonds,[1] and their reactions with a wide variety of substrates have produced some very interesting results.[2] Another important facet of polyhydride complexes is the rapidly expanding area of η^2-dihydrogen complexes, and it has been shown that many polyhydride complexes are actually mixed hydride/η^2-dihydrogen complexes.[3] Since Chatt and Coffey first characterized $ReH_7(PPh_3)_2$ in 1966,[4] it has become one of the most studied transition metal polyhydride complexes.

Crabtree[5a] and Walton[5b] have classified the heptahydride as formally being a Re(V) dihydrogen complex by T_1 measurements and electrochemistry, respectively.[6] The heptahydride thermally loses H_2 to produce the unsaturated 16-electron intermediate [$ReH_5(PPh_3)_2$], which can then react with simple 2- or 4-electron donor ligands to form adducts of the type $ReH_5(PPh_3)_2L$[7,8] or $ReH_3(PPh_3)_2(LL)$[8] or it can react further to hydrogenate 3,3-dimethyl-1-butene and produce the highly reactive 14-electron intermediate [$ReH_3(PPh_3)_2$].[9,10b] Therefore, if the 4-electron donor is a diene, this intermediate can bind directly to the diene fragment, and it is possible to observe, and sometimes isolate, complexes such as (η^4-diene)$ReH_3(PPh_3)_2$, (η^5-pentadienyl)-$ReH_2(PPh_3)_2$, and (η^6-arene)$ReH(PPh_3)_2$.[10]

There is a lot of interest in transition metal indenyl complexes due to their greatly enhanced reactivity over their corresponding cyclopentadienyl analogs. This "indenyl ligand effect"[11] is seen for both associative[12,13] and dissociative[13c,14] ligand substitution reactions, although the associative effect is by far the strongest, giving rate enhancements of up to 10^8 times faster than that of the analogous cyclopentadienyl complex.[15] We wished to synthesize (η^5-C_9H_7)$ReH_2(PPh_3)_2$ in order to compare its reactivity with that of (η^5-C_5H_5)$ReH_2(PPh_3)_2$, which is known to undergo both photochemical ligand exchange and activation of aromatic and aliphatic C–H bonds,[16] in order to determine whether or not the chemistry observed with the Cp compound is due in any part to an η^5–η^3 ring slippage. If ring slippage is occurring in the Cp compound, then the indenyl compound should show a similar reactivity at a much greater rate.

In a reaction analogous to that for the preparation of the cyclopentadienyl complex, $ReH_7(PPh_3)_2$ was reacted with an excess of indene and related indene derivatives. In this article,

(1) Parshall, G. W. *Acc. Chem. Res.* **1975**, *8*, 113.
(2) Baudry, D.; Daran, J. C.; Dromzee, Y.; Ephritikhine, M.; Felkin, H.; Jeannin, Y.; Zakrzewski, J. *J. Chem. Soc., Chem. Commun.* **1983**, 813.
(3) Kubas, G. J. *Acc. Chem. Res.* **1988**, *21*, 120.
(4) Chatt, J.; Coffey, R. S. *J. Chem. Soc., Chem. Commun.* **1966**, 545.
(5) (a) Hamilton, D. G.; Crabtree, R. H. *J. Am. Chem. Soc.* **1988**, *110*, 4126. (b) Costello, M. T.; Walton, R. A. *Inorg. Chem.* **1988**, *27*, 2563.
(6) An X-ray crystal structure of $ReH_7(PPh_3)_2$ has been done, but the hydrides were not located. Howard, J. A. K.; Mead, K. A.; Spencer, J. L. *Acta Crystallogr.* **1983**, *C39*, 555. However, a neutron diffraction study has been done on the very similar $ReH_7[P(o\text{-tolyl})_3]_2$, and it was found to have a long H_2 interaction of 1.36 Å. Brammer, L.; Howard, J. A.; Johnson, O.; Koetzle, T. F.; Spencer, J. L.; Stringer, A. M. *J. Chem. Soc., Chem. Commun.* **1991**, 241.
(7) (a) Chatt, J.; Coffey, R. S. *J. Chem. Soc. A* **1969**, 1963. (b) Allison, J. D.; Moehring, G. A.; Walton, R. A. *J. Chem. Soc., Dalton Trans.* **1986**, 67.
(8) Moehring, G. A.; Walton, R. A. *Inorg. Chem.* **1987**, *26*, 2910.
(9) Green, M. A.; Huffman, J. C.; Caulton, K. G.; Kybak, W. K.; Ziolkowski, J. J. *J. Organomet. Chem.* **1981**, *218*, C39.
(10) (a) Baudry, D.; Ephritikhine, M.; Felkin, H. *J. Organomet. Chem.* **1982**, *224*, 363. (b) Baudry, D.; Ephritikhine, M.; Felkin, H.; Jeannin, Y.; Robert, F. *J. Organomet. Chem.* **1981**, *220*, C7. (c) Jones, W. D.; Maguire, J. A. *Organometallics* **1987**, *6*, 1301. (d) Jones, W. D.; Maguire, J. A. *Organometallics* **1985**, *4*, 951. (e) Baudry, D.; Ephritikhine, M.; Felkin, H. *J. Chem. Soc., Chem. Commun.* **1980**, 1243.
(11) Rerek, M. E.; Ji, L.-N.; Basolo, F. *J. Chem. Soc., Chem. Commun.* **1983**, 1208.
(12) O'Connor, J. M.; Casey, C. P. *Chem. Rev.* **1987**, *87*, 307 and references therein.
(13) (a) Kakkar, A. K.; Taylor, N. J.; Marder, T. B. *Organometallics* **1989**, *8*, 1765. (b) Nabib, A.; Tanke, R. S.; Holt, E. M.; Crabtree, R. H. *Organometallics* **1989**, *8*, 1225. (c) Turaki, N. N.; Huggins, J. M.; Lebioda, L. *Inorg. Chem.* **1988**, *27*, 424.
(14) (a) White, C.; Mawby, R. J. *Inorg. Chim. Acta* **1970**, *4*, 261. (b) White, C.; Mawby, R. J.; Hart-Davis, A. J. *Inorg. Chim. Acta* **1970**, *4*, 441. (c) Jones, D. J.; Mawby, R. J. *Inorg. Chim. Acta* **1972**, *6*, 157.
(15) Rerek, M. E.; Basolo, F. *J. Am. Chem. Soc.* **1984**, *106*, 5908.
(16) Jones, W. D.; Maguire, J. A. *Organometallics* **1986**, *5*, 590.

0002-7863/93/1515-965$04.00/0

Table I. NMR Spectroscopic Data for Complexes **1**, **2**, **5–8**, and **10** in C_6D_6

	^{1}H NMR, ppm	^{13}C{^{1}H} NMR, ppm[a]	^{31}P{^{1}H} NMR, ppm
1	7.46 (dd, J = 8.1, 7.5 Hz, 12 H), 6.95 (m, 18 H), 6.78 (dd, J = 6.7, 3.1 Hz, 2 H), 6.56 (dd, J = 6.7, 3.0 Hz, 2 H), 4.60 (t, J = 2.3 Hz, 1 H), 4.54 (d, J = 2.3 Hz, 2 H), −9.85 (t, J = 41.3 Hz, 2 H)	143.68 (d, J = 50.3 Hz, C_{ipso}), 134.13 (t, J = 4.6 Hz, C_{ortho}), 128.48 (s, C_{para}), 127.19 (t, J = 4.6 Hz, C_{meta}), 126.50 (s), 124.30 (s), 110.50 (s), 74.80 (s), 71.56 (s)	34.6 (br s)
2	7.80 (dd, J = 9.3, 7.6 Hz, 6 H), 7.66 (dd, J = 9.3, 7.6 Hz, 6 H), 6.95 (m, 18 H), 4.16 (dq, J = 9.6, 5.9 Hz, 1 H, H^1), 3.62 (br d, J = 6.3 Hz, 1 H, H^2), 3.16 (ddt, J = 14.0, 9.8, 2.9 Hz, 1 H, H^3), 3.12 (dd, J = 14.0, 8.4 Hz, 1 H, H^4), 2.94 (dt, J = 9.4, 5.5 Hz, 1 H, H^5), 2.64 (br dd, J = 6.3, 5.5 Hz, 1 H, H^6), 2.46 (ddd, J = 14.5, 10.6, 7.6 Hz, 1 H, H^7), 2.36 (br d, J = 5.8 Hz, 1 H, H^8), 2.29 (m, 1 H, H^9), 1.80 (dt, J = 11.8, 7.5 Hz, 1 H, H^{10}), 1.13 (dd, J = 14.5, 7.7 Hz, 1 H, H^{11}), −2.66 (dddd, J = 41.5, 31.7, 10.1, 5.4 Hz, 1 H, H^{12}), −11.26 (dddd, J = 40.0, 34.0, 10.3, 3.1 Hz, 1 H, H^{13})	141.20 (d, J = 40.0 Hz, C_{ipso}), 140.30 (d, J = 40.0 Hz, $C_{ipso'}$), 134.80 (s, C_{ortho}), 134.50 (s, $C_{ortho'}$), 128.54 (s, $C_{para,para'}$), 127.20 (s, $C_{meta,meta'}$), 103.80 (s, C^9), 101.20 (d, J = 5.5 Hz, C^8), 82.53 (d, J = 5.5 Hz, C^4), 33.80 (s, C^3), 32.20 (s, C_6), 31.00 (s, C^1), 25.70 (dd, J = 9.0, 2.4 Hz, C^7), 25.32 (dd, J = 9.0, 2.1 Hz, C^5), 24.63 (s, C^2)	32.2 (br s, P^1) 27.7 (br s, P^2)
5	7.79 (ddd, J = 10.4, 8.4, 1.4 Hz, 6 H), 6.95 (m, 9 H), 4.92 (br dd, J = 3.3, 2.0 Hz, 2 H), 4.54 (dd, J = 3.3, 2.0 Hz, 2 H), 2.49 (ddd, J = 14.5, 10.4, 7.8 Hz, 2 H), 2.23 (dd, J = 14.5, 7.8 Hz, 2 H), 1.91 (m, 1 H), 1.46 (dt, J = 12.0, 7.8 Hz, 1 H), −8.03 (d, J = 26.7 Hz, 3 H)	133.85 (d, J = 11.3 Hz, C_{ortho}), 128.29 (s, C_{para}), 127.54 (d, J = 9.0 Hz, C_{meta}), 84.30 (s), 72.26 (d, J = 1.7 Hz), 32.43 (s), 24.95 (s)	35.2 (br s)
6	7.60 (t, J = 7.6 Hz, 12 H), 6.96 (m, 18 H), 4.55 (br dd, J = 3.6, 2.0 Hz, 2 H), 3.57 (br dd, J = 3.6, 2.0 Hz, 2 H), 2.62 (ddd, J = 13.2, 11.1, 6.9 Hz, 2 H), 2.48 (m, 1 H), 2.2 (dd, J = 13.2, 6.9 Hz, 2 H), 1.77 (dt, J = 11.1, 6.9 hz, 1 H), −7.21 (t, J = 33.9 Hz, 1 H)	134.37 (t, J = 5.1 Hz, C_{ortho}), 127.95 (s, C_{para}), 126.93 (t, J = 4.2 Hz, C_{meta}), 72.93 (s), 72.01 (pt, J = 2.5 Hz), 31.49 (s), 25.07 (s)	27.4 (br s)
7	7.85 (m, 12 H), 6.99 (m, 18 H), 3.80 (br m, 2 H), 3.3 (br d, J = 4.2 Hz, 2 H), 1.84 (m, 1 H), 1.83 (m, 2 H), 1.40 (m, 2 H), 1.26 (m, 2 H), 1.25 (m, 1 H), −5.73 (br s, 3 H)	134.52 (t, J = 5.2 Hz, C_{ortho}), 127.98 (s, C_{para}), 127.62 (t, J = 4.6 Hz, C_{meta}), 70.77 (s), 59.53 (s), 44.71 (s), 37.84 (s), 27.07 (s)	32.2 (br s)
8	7.69 (t, J = 8.1 Hz, 12 H), 6.96 (m, 18 H), 4.5 (br t, J = 2.3 Hz, 1 H), 3.95 (br d, J = 2.3 Hz, 2 H), 2.14 (m, 4 H), 1.56 (m, 2 H), 1.27 (m, 2 H), −9.72 (t, J = 40.3 Hz, 2 H)	134.31 (t, J = 5.1 Hz, C_{ortho}), 128.31 (s, C_{para}), 127.20 (t, J = 4.2 Hz, C_{meta}), 78.81 (t, J = 1.9 Hz), 71.46 (t, J = 1.1 Hz), 24.01 (s), 23.61 (s)	36.6 (br s)
10	7.49 (dd, J = 9.7, 7.8 Hz, 12 H), 7.01 (br t, J = 7.5 Hz, 12 H), 6.86 (t, J = 7.3 Hz, 6 H), 5.98 (dd, J = 4.4, 2.3 Hz, 2 H), 4.53 (br dd, J = 4.4, 2.3 Hz, 2 H), 2.09 (m, 2 H), 1.45 (m, 3 H), 1.35 (m, 1 H), −7.95 (t, J = 37.8 Hz, 2 H)	133.99 (t, J = 5.1 Hz, C_{ortho}), 129.92 (s, C_{para}), 128.29 (s, C_{meta}), 91.79 (br s), 90.75 (br s), 30.23 (s), 24.27 (s)	23.2 (br s)

[a] The reported ^{13}C{^{1}H} NMR spectra of **5–8** and **10** were acquired as ^{13}C DEPT spectra, so the ipso carbons are not observed.

we report the surprising results of this reaction and discuss the characterization and reactivity of the complexes obtained, along with the mechanism for their formation.

Results and Discussion

Preparation of (η^5-C_9H_7)$ReH_2(PPh_3)_2$ (1) and (η^5-C_9H_{11})-$ReH_2(PPh_3)_2$ (2). The reaction of $ReH_7(PPh_3)_2$ with an excess of indene in either benzene or tetrahydrofuran as solvent yields a mixture of two organometallic complexes (eq 1), the ratio of which is dependent on the reaction conditions employed (see below). Due to the great similarity between the two complexes,

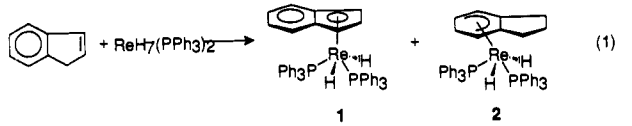

(1)

separation could not be achieved and alternative reactions were required to obtain the two compounds in pure form. The minor product was easily identified as (η^5-C_9H_7)$ReH_2(PPh_3)_2$ (**1**) from its spectroscopic data (Table I). The ^{1}H NMR data indicates that there are three Cp-like protons in a 2:1 ratio, along with two pairs of unbound olefinic protons. The upfield triplet at δ −9.85 indicates the presence of two equivalent metal hydrides which are coupled to two equivalent phosphorus atoms. This formulation is also consistent with the ^{31}P{^{1}H} NMR spectrum, which exhibits a broad singlet indicating equivalent phosphorus atoms.

Compound **1** is the simple indenyl analog of the known compound (η^5-C_5H_5)$ReH_2(PPh_3)_2$[10,16] (Figure 1) and was the expected product of the reaction on the basis of the known reaction of $ReH_7(PPh_3)_2$ with cyclopentadiene. The solid-state structure of **1** obtained by single-crystal X-ray diffraction confirmed this assignment (Figure 2). Selected bond lengths and angles for **1**

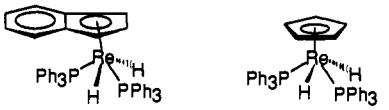

Figure 1. Comparison of indenyl and cyclopentadienyl complexes.

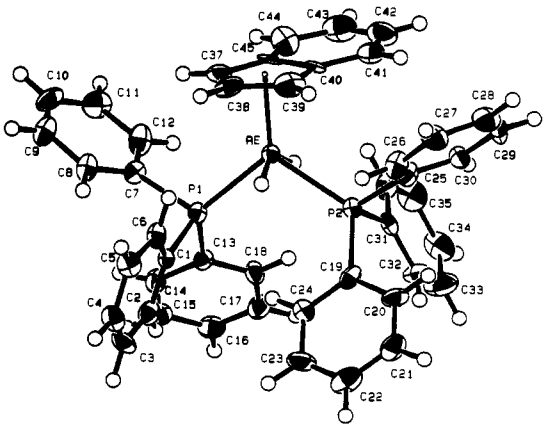

Figure 2. ORTEP diagram of **1** with the thermal ellipsoids shown at 50% probability. The hydride ligands were located and refined.

are listed in Table II. The crystal structure shows that **1** is indeed analogous to the Cp compound and that there is very little distortion of the indene toward an η^3 binding mode. The Re–P and Re–H bond lengths are almost identical to those of the Cp compound.[10c] The carbon atoms of the five-membered ring are planar to within 0.0125 Å, and the Re–C bond distances for the η^5-indene ligand are 2.28 (1), 2.23 (1), 2.23 (1), 2.327 (8), and 2.385 (9)

Table II. Selected Bond Distances (Å) and Angles (deg) for $(\eta^5\text{-}C_9H_7)Re(PPh_3)_2H_2$ (**1**)

Bond Distances			
Re–P(1)	2.318 (3)	C(37)–C(45)	1.42 (1)
Re–P(2)	2.329 (3)	C(38)–C(39)	1.46 (2)
Re–C(37)	2.28 (1)	C(39)–C(40)	1.43 (1)
Re–C(38)	2.23 (1)	C(40)–C(41)	1.43 (1)
Re–C(39)	2.23 (1)	C(40)–C(45)	1.46 (1)
Re–C(40)	2.327 (8)	C(41)–C(42)	1.33 (2)
Re–C(45)	2.385 (9)	C(42)–C(43)	1.41 (2)
Re–H(38)	1.5 (1)	C(43)–C(44)	1.36 (2)
Re–H(39)	1.5 (1)	C(44)–C(45)	1.40 (1)
C(37)–C(38)	1.40 (1)		
Bond Angles			
P(1)–Re–P(2)	107.0 (1)	P(2)–Re–H(38)	70 (4)
P(1)–Re–H(38)	86 (4)	P(2)–Re–H(39)	79 (4)
P(1)–Re–H(39)	81 (3)	H(38)–Re–H(39)	141 (5)

Table III. Selected Bond Distances (Å) and Angles (deg) for $(\eta^5\text{-}C_9H_{11})ReH_2(PPh_3)_2$ (**2**)

Bond Distances			
Re–P(1)	2.366 (8)	C(30)–C(41)	1.37 (4)
Re–P(2)	2.36 (1)	C(40)–C(45)	1.33 (5)
Re–C(40)	2.33 (3)	C(41)–C(42)	1.38 (5)
Re–C(41)	2.25 (4)	C(42)–C(43)	1.46 (4)
Re–C(42)	2.15 (3)	C(43)–C(44)	1.50 (5)
Re–C(44)	2.20 (2)	C(44)–C(45)	1.40 (4)
Re–C(45)	2.27 (3)		
Bond Angle			
P(1)–Re–P(2)	103.9 (3)		

Å (those for the Cp compound range from 2.22 to 2.30 Å). The angle between the plane of the allyl carbons (C37, C38, C39) and that of the four-carbon unit (C37, C39, C40, C45) is only 2.51°. This angle is a measure of the degree of ring slippage, and it is among the smallest that has been measured,[17] indicating very little slippage toward an η^3 binding mode. The six-membered ring is planar to within 0.012 Å, and it is bent an additional 3.1° away from the four-carbon unit. The diene unit in the six-membered ring is localized to C41–C42 (1.33 Å) and C43–C44 (1.36 Å).

The major product of the reaction, **2**, displayed a much more complex ^1H NMR spectrum (Table I), consisting of 11 distinct resonances between δ 4.2 and 1.1 plus aromatic PPh_3 resonances and two inequivalent hydride resonances upfield at δ −2.66 and −11.26. The $^{31}P\{^1H\}$ NMR spectrum shows two inequivalent phosphorus atoms at δ 32.14 and 27.63. A ^{13}C DEPT NMR spectrum showed the presence of four methylene carbon atoms, and further characterization by ^1H–^1H COSY and ^{13}C–^1H HETCOR allowed the formulation of the major product as $(\eta^5\text{-}C_9H_{11})ReH_2(PPh_3)_2$ (**2**). The complex contains an η^5-indanyl ligand, in which a molecule of indene has been partially hydrogenated and the metal has migrated from the five- to the six-membered ring. This binding mode for indan has been postulated as one of the anionic intermediates in the reaction of $(\eta^6\text{-indan})Cr(CO)_3$ with nucleophiles,[18] and it has also been seen in the cationic complexes formed upon the abstraction of a hydride from $(\eta^4\text{-}5,6\text{-dihydroindan})Fe(CO)_3$.[19]

The solid-state structure of **2** obtained by single-crystal X-ray diffraction confirmed this assignment (Figure 3). Selected bond lengths and angles for **2** are listed in Table III. The five carbon

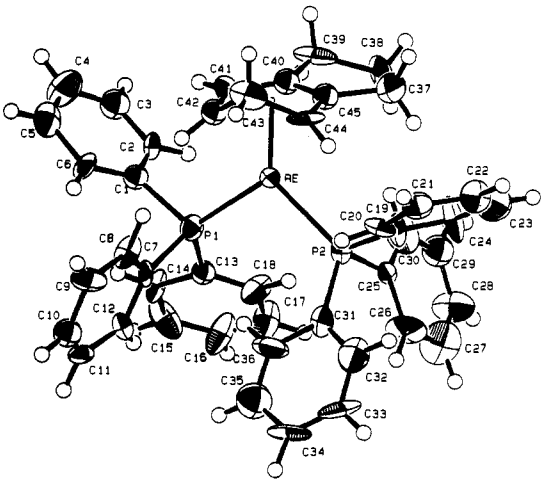

Figure 3. ORTEP diagram of **2** with the thermal ellipsoids shown at 50% probability. The hydride ligands were not located.

Scheme I. Proposed Mechanism for the Formation of **1** and **2**

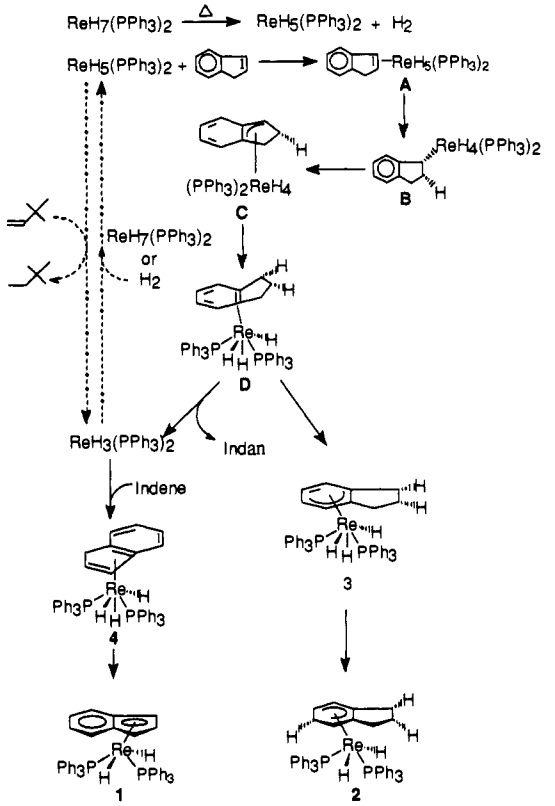

atoms that are bound to Re are planar to within 0.01 Å. The methylene carbon C43 is bent out of the plane away from the Re atom by 49°. The endo proton on C43 (H40) lies 3.3 Å from Re. The C43 methylene group lies in a plane bisecting the plane formed by P1, Re, and P2 (the dihedral angle between these planes is 95.0°). This geometry helps explain the couplings that are seen in the ^1H and ^{13}C NMR spectra since it places P1 trans to C44–C45 and P2 trans to C41–C42. The hydrides would then lie trans to the endo protons on C43 and C39.

Proposed Mechanism for the Formation of 1 and 2. A plausible mechanism for the reaction of $ReH_7(PPh_3)_2$ with indene leading to the formation of **1** and **2** is proposed in Scheme I. The heptahydride first loses H_2 and then reacts with indene to form intermediate **A**. The indene is then intramolecularly hydrogenated (**B** and **C**) to form the 16-electron η^2-bound indan intermediate **D**. This compound can then either ring slip to an η^4-bound indan to form **3** (now an 18-electron complex) or lose indan to produce $ReH_3(PPh_3)_2$, which would then react with a second molecule of

(17) The angle is Ω as defined in Faller, J. W.; Crabtree, R. H.; Habib, A. *Organometallics* **1985**, *4*, 929.

(18) (a) Ohlsson, B.; Ullenius, C.; Jagner, S.; Grivet, C.; Wenger, E.; Kündig, E. P. *J. Organomet. Chem.* **1989**, *365*, 243. (b) Jackson, W. R.; Rae, I. D.; Wong, M. G. *Aust. J. Chem.* **1986**, *39*, 303. (c) Boutonnet, J. C.; Mordenti, L.; Rose, E.; Le Martret, O.; Precigoux, G. *J. Organomet. Chem.* **1981**, *221*, 147. (d) Jackson, W. R.; Rae, I. D.; Wong, M. G.; Semmelhack, M. F.; Garcia, J. N. *J. Chem. Soc., Chem. Commun.* **1982**, 1359.

(19) Birch, A. J.; Bandara, B. M. R.; Chamberlain, K.; Chauncy, B.; Dahler, P.; Day, A. I.; Jenkins, I. D.; Kelly, L. F.; Khor, T. C.; Kretschmer, G.; Liepa, A. J.; Narula, A. S.; Raverty, W. D.; Rizzardo, E.; Sell, C.; Stephenson, G. R.; Thompson, D. J.; Williamson, D. H. *Tetrahedron* **1981**, *37*, 289.

indene to form **4**. The migration of a hydride in **3** from the metal center to the 5 position of the bound indan ring results in the formation of **2**, while the loss of H_2 from **4**, followed by subsequent hydrogen migration from the η^4-bound indene to the metal center, results in the formation of **1**.[20] This latter process is precisely what is seen for the cyclopentadienyl analog of **4**.[10]

To test the intramolecularity of the hydride migrations that take place during the formation of **2**, $ReD_7(PPh_3)_2$ was used in place of $ReH_7(PPh_3)_2$. If the migrations are intramolecular and the symmetric intermediate **D** indeed lies on the reaction pathway, one would expect to see complete deuteration of H_5 and H_9 and a scrambling of the label at H_4 and H_{11}, resulting in 50% deuteration at these sites. Reaction of $ReD_7(PPh_3)_2$ with an excess of indene in C_6D_6 gives exactly this deuterium distribution, and it supports the steps leading to the formation of **D**.

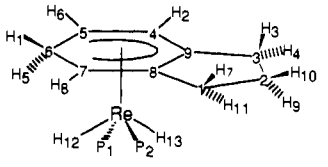

Numbering Scheme for **2**

In order to further test the proposed mechanism, 3,3-dimethyl-1-butene was added to the reaction prior to indene addition. Now the $[ReH_5(PPh_3)_2]$ formed after the initial H_2 loss hydrogenates the 3,3-dimethyl-1-butene to produce the highly reactive $[ReH_3(PPh_3)_2]$.[9,10b] This species should then react with indene and lead to the direct formation of **4**. The hydrogenation of 3,3-dimethyl-1-butene competes with the direct reaction of $[ReH_5(PPh_3)_2]$ with indene and therefore shuts down the formation of **2**. This is precisely what was seen. When $ReH_7(PPh_3)_2$ was reacted with 3,3-dimethyl-1-butene (0.42 M) and indene (0.28 M) in THF, **1** was the major product (the ratio of **1** to **2** was 11:1).

There was no direct evidence for the formation of **4** at any time during the reaction (either with or without 3,3-dimethyl-1-butene). This observation was in contrast with the analogous reaction with cyclopentadiene in which the η^4-bound cyclopentadiene complex is stable and isolable.[10c] Presumably, the intramolecular hydride migration in **4** is very rapid since there is a concurrent gain in resonance stabilization energy of up to 1.16β or roughly 21 kcal/mol (based on the β values for indene and the indenyl anion), compared to the 14 kcal/mol gained for the Cp analog (based on the β values for cyclopentadiene and the cyclopentadienyl anion).[21]

There is, however, spectroscopic evidence for the formation of **3** during the reaction, but it is not isolable. If the reaction is followed by ^1H NMR spectroscopy, resonances attributable to **3** are seen to grow in and then diminish as the reaction proceeds. These resonances are also seen to appear when a sample of **2** is heated, suggesting that the migration is reversible (vide infra).

Kinetic Study of the Reaction of $ReH_7(PPh_3)_2$ and Indene. A study was undertaken to determine whether or not the reaction was dependent on the concentration of either indene or $ReH_7(PPh_3)_2$. In the first experiment, three NMR samples were prepared from a stock solution of 0.034 M $ReH_7(PPh_3)_2$ to which *n*-pentane (0.093 M) was added as an internal standard. Aliquots of indene were then added to each sample (0.09, 0.38, and 1.22 M). The reaction was monitored at room temperature by ^1H NMR spectroscopy by integrating the hydride resonances of $ReH_7(PPh_3)_2$ and **1**–**3**. It was found that the concentration of the indene had no effect on either the rate of disappearance of $ReH_7(PPh_3)_2$ (found to be $3.10(6) \times 10^{-5}$ s^{-1}) or on the ratio of products formed, **2**:**1** = 9:1.

In the second experiment, two NMR samples were prepared with equal concentrations of indene (0.40 M) and *n*-pentane (0.093 M). $ReH_7(PPh_3)_2$ was then added to the two samples (0.037 and 0.005 M). The reaction was monitored as before, and the results were surprising. It was found that the concentration of the $ReH_7(PPh_3)_2$ had no effect on the rate of disappearance of $ReH_7(PPh_3)_2$ (as expected), but there *was* an effect on the product ratio. The ratio of **2** to **1** increased with increasing $[ReH_7(PPh_3)_2]$. The reason for this was not readily apparent from the proposed mechanism in Scheme I, in which one would predict no $ReH_7(PPh_3)_2$ dependence. Upon further examination, it was proposed that the $[ReH_3(PPh_3)_2]$ formed upon loss of indan from intermediate **D** can also react with either $ReH_7(PPh_3)_2$ or H_2 that is free in solution to form more $[ReH_5(PPh_3)_2]$. Therefore, the formation of **1** is inhibited by excess $ReH_7(PPh_3)_2$ or H_2 by the trapping out of the reactive $[ReH_3(PPh_3)_2]$. One must now question the initial step proposed in Scheme I.

Baudry and co-workers have previously proposed the same dihydride transfer from $ReH_7(PPh_3)_2$ to$[ReH_3(PPh_3)_2]$ in the reaction of $ReH_7(PPh_3)_2$ with cyclopentane in the presence of excess 3,3-dimethyl-1-butene.[10e] They also found only a trace (<0.2 equiv) of free H_2 and suggested that only a small amount of the starting $ReH_7(PPh_3)_2$ actually loses H_2. The remaining $ReH_7(PPh_3)_2$ can be converted into $[ReH_5(PPh_3)_2]$ and $[ReH_3(PPh_3)_2]$ in a series of reactions in which 3,3-dimethyl-1-butene is hydrogenated (they detected 4.5 equiv of 2,2-dimethylbutane). Upon closer examination of our reaction, we found that only 0.15 equiv of free H_2 (based on the amount of **1** that was formed) was observed by ^1H NMR spectroscopy. Surely, both $ReH_7(PPh_3)_2$ and H_2 can react with $[ReH_3(PPh_3)_2]$ to form $[ReH_5(PPh_3)_2]$, but the question of how much $ReH_7(PPh_3)_2$ initially loses H_2 is unclear since the free H_2 would be quickly scavenged by $[ReH_3(PPh_3)_2]$. Only 1.7 equiv of free indan was observed compared to the 4.6 equiv of **2** that was formed, suggesting that intermediate **D** rearranges to **3** faster than it loses free indan.

To test the proposal that free H_2 can react with $[ReH_3(PPh_3)_2]$, an experiment was run in which two NMR samples were prepared with equal concentrations of $ReH_7(PPh_3)_2$ (0.034 M) and indene (0.40 M). One of the samples was then placed under an atmosphere of H_2, and the product ratios of both samples were examined after 48 h. The sample without H_2 had a product ratio of **2**:**1** = 8, while the sample with added H_2 had a product ratio of **2**:**1** = 65! Therefore, running the reaction under an atmosphere of H_2 provides ideal reaction conditions for obtaining pure **2**.

Photochemistry of 1. We were interested in the photochemistry of **1** since its Cp analog is a photocatalyst for the activation of C–H bonds.[16] Two samples were made of a solution of **1** (5 mg) in C_6D_6 with either excess PMe_3 (100 equiv), or *n*-pentane as a substrate to test **1** for phosphine exchange and H/D exchange, respectively, both of which occur photochemically with the Cp complex. These samples were irradiated using a $\lambda > 345$ nm filter, and the reaction was monitored by ^1H and ^2H NMR spectroscopy. It was found that there was no reaction occurring in either of these samples. Irradiation was then conducted without the use of a filter (which results in rapid decomposition of the Cp compound), and again there was no reaction (and no decomposition). Apparently, the indenyl complex does not undergo the same photochemistry as $CpReH_2(PPh_3)_2$.

Thermal Chemistry of 1. Since indenyl complexes are generally more reactive than their Cp analogs, we chose to study the thermal chemistry of **1** even though $CpReH_2(PPh_3)_2$ is thermally stable up to 220 °C.[22] Three samples of **1** in toluene-d_8 with excess PMe_3 were heated to 50, 100, and 150 °C, and the reaction was monitored by ^1H NMR spectroscopy. No reaction was seen for

(20) (a) Similar intermediates have been previously proposed for an iridium system. Crabtree, R. H.; Parnell, C. P. *Organometallics* **1984**, *3*, 1727. For other examples of haptomeric equilibria, see: (b) Brammer, L.; Howard, J. A. K.; Johnson, O.; Koetzle, T. F.; Spencer, J. L.; Stringer, A. M. *J. Chem. Soc., Chem. Commun.* **1991**, 241. (c) White, C.; Thompson, S. J.; Maitlis, P. M. *J. Chem. Soc., Dalton Trans.* **1977**, 1654. (d) Treichel, P. M.; Fiviz-zani, K. P.; Haller, K. J. *Organometallics* **1982**, *1*, 931. (e) Albright, T. A.; Hofmann, P.; Hoffmann, R.; Lillya, C. P.; Dobosh, P. A. *J. Am. Chem. Soc.* **1983**, *105*, 3396. (f) Ustynyuk, N. A.; Loshin, B. V.; Oprunenko, Yu. F.; Roznyatovsky, V. A.; Luzikov, Yu. N.; Ustynyuk, Yu. A. *J. Organomet. Chem.* **1980**, *202*, 279.

(21) Coulson, C. A.; Streitwieser, A., Jr. *Dictionary of π-Electron Calculations*; W. H. Freeman and Company: San Francisco, 1965.

(22) Maguire, J. A. Ph.D. Thesis, University of Rochester, Rochester, NY, 1986, p 99.

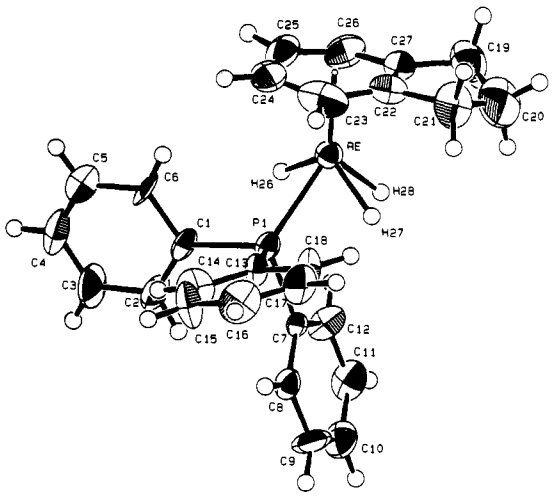

Figure 4. ORTEP diagram of **5** with the thermal ellipsoids shown at 50% probability. The hydride ligands were located and refined.

Table IV. Selected Bond Distances (Å) and Angles (deg) for $Re(\eta^6\text{-}C_9H_{10})H_3PPh_3$ (**5**)

	Bond Distances		
Re–P(1)	2.300 (4)	Re–H(27)	1.6 (1)
Re–C(22)	2.31 (2)	Re–H(28)	1.6 (1)
Re–C(23)	2.25 (2)	C(22)–C(23)	1.45 (2)
Re–C(24)	2.31 (2)	C(22)–C(27)	1.41 (2)
Re–C(25)	2.27 (2)	C(23)–C(24)	1.45 (2)
Re–C(26)	2.19 (1)	C(24)–C(25)	1.39 (2)
Re–C(27)	2.30 (2)	C(25)–C(26)	1.39 (2)
Re–H(26)	1.8 (1)	C(26)–C(27)	1.41 (2)
	Bond Angles		
P(1)–Re–H(26)	70 (3)	H(26)–Re–H(27)	115 (5)
P(1)–Re–H(27)	67 (4)	H(26)–Re–H(28)	81 (5)
P(1)–Re–H(28)	92 (4)	H(27)–Re–H(28)	55 (5)

the samples at 50 and 100 °C. At 150 °C, however, several species were observed to have grown in. Phosphine exchange was indeed occurring (both $(\eta^5\text{-}C_9H_7)ReH_2(PPh_3)(PMe_3)$ and $(\eta^5\text{-}C_9H_7)\text{-}ReH_2(PMe_3)_2$ were observed by ^1H NMR spectroscopy), but there was also substantial formation of the known[23] $HRe(PMe_3)_5$. No evidence for H/D exchange between C_6D_6 and *n*-pentane was seen.

Photochemistry of 2: Preparation of $(\eta^6\text{-}C_9H_{10})ReH_3(PPh_3)$ (5). Photolysis of a solution of **2** in C_6D_6 results in the disappearance of the ^1H NMR resonances of **2**, along with the concurrent appearance of resonances for free PPh_3 and a single new organometallic product **5** (eq 2). The ^1H NMR spectrum of this

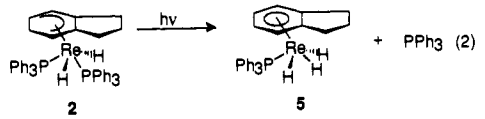

2 **5**

new product exhibits an upfield doublet at δ −8.03, which integrates as three hydrides and indicates that there is now only one triphenylphosphine bound to the metal. The six ^1H resonances between δ 1.46 and 4.92 and their coupling patterns are consistent with the presence of a symmetrically bound indan ligand and allow the formulation of the complex as $(\eta^6\text{-}C_9H_{10})ReH_3(PPh_3)$ (**5**) (Table I). This formulation was confirmed by single-crystal X-ray diffraction (Figure 4). Selected bond lengths and angles for **5** are listed in Table IV. The six carbon atoms that are bound to Re are planar to within 0.04 Å. This complex is the indan analog of the known η^6-benzene complex $(\eta^6\text{-}C_6H_6)ReH_3(PPh_3)$.[24]

The room-temperature ^1H NMR spectrum of **5** indicates three equivalent hydrides, but the hydrides are actually inequivalent (the crystal structure shows two cis to the phosphine and one trans). Therefore, a low-temperature ^1H NMR study was conducted in an attempt to resolve the two types of hydrides. A sample of **5** in THF-d_8 was slowly cooled to 165 K in the probe of the NMR spectrometer, and the ^1H resonance of the hydride at δ −8.647 (d, J = 26.9 Hz, 3 H) was monitored. The resonance was seen to gradually broaden and then finally coalesce at 185 K. The hydrides were finally resolved at 170 K into a broad singlet at δ −7.992 (1 H) and a doublet at δ −9.374 (J = 40.1 Hz, 2 H). This corresponds to a $\Delta G^{\ddagger}$ value of 8.03 kcal/mol for the interconversion of the three hydrides at 185 K.

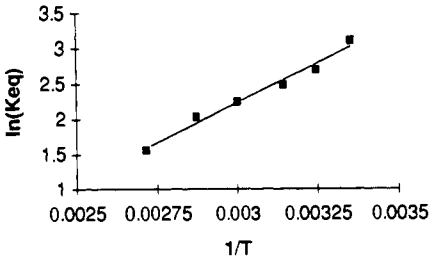

Figure 5. Plot of ln (K_{eq}) vs $1/T$ for the equilibration of **2** and **3**.

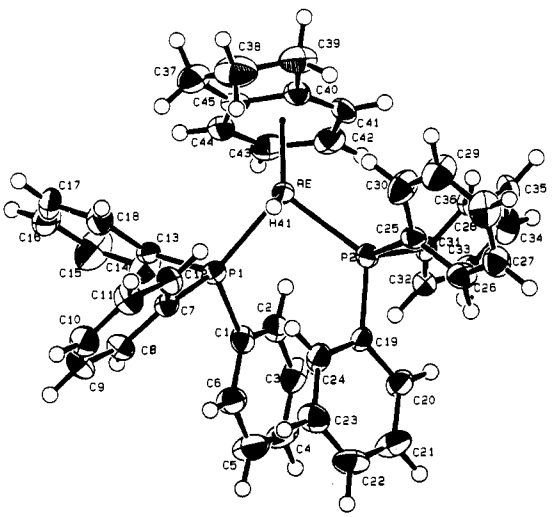

Figure 6. ORTEP diagram of **6** with the thermal ellipsoids shown at 50% probability. The hydride ligand was located and refined.

Thermal Chemistry of 2: (a) The Interconversion of 2 and 3. When a solution of **2** in toluene-d_8 is heated, the ^1H NMR spectrum shows the growth of the resonances attributed to **3**, with a concurrent decrease in the resonances of **2**. If the same solution is then allowed to cool, the resonances due to **3** decrease and those of **2** return to their original height. This temperature-dependent equilibrium was then studied in toluene-d_8 in order to determine the activation parameters of the hydride migration. A van't Hoff plot for the equilibrium (Figure 5) with K = [**2**]/[**3**] gives ΔH° = −4.4 (0.3) kcal/mol and ΔS° = −8.7 (0.9) cal/mol·K.

(b) Preparation of $(\eta^6\text{-}C_9H_{10})ReH(PPh_3)_2$ (6). Prolonged heating of the mixture of **2** and **3** at elevated temperatures results in the irreversible loss of H_2 from **3** and the formation of a single new organometallic product **6** (eq 3). The ^1H NMR spectrum

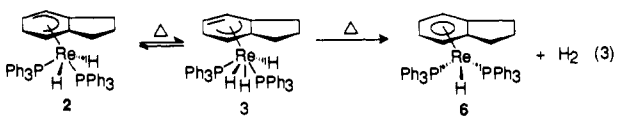

2 **3** **6**

of this product shows a new upfield triplet at δ −7.206, which integrates as one proton, and indicates the presence of two phosphine ligands. The six ^1H resonances between δ 4.75 and 1.75 and their coupling patterns are again consistent with an η^6-bound indan ligand and allow the formulation of the complex as $(\eta^6\text{-}C_9H_{10})ReH(PPh_3)_2$ (**6**) (Table I). This formulation was confirmed by single-crystal X-ray diffraction (Figure 6). Selected bond lengths and angles for **6** are listed in Table V. The six carbon atoms that are bound to Re are planar to within 0.016 Å. The

(23) Jones, W. D.; Maguire, J. A. *Organometallics* **1987**, *6*, 1728.
(24) Jones, W. D.; Fan, M. *Organometallics* **1986**, *5*, 1057.

Table V. Selected Bond Distances (Å) and Angles (deg) for (η^6-indan)Re(PPh_3)$_2$H (6)

Bond Distances			
Re-P(1)	2.339 (2)	Re-H(41)	1.70 (5)
Re-P(2)	2.355 (2)	C(40)-C(41)	1.380 (8)
Re-C(40)	2.250 (6)	C(40)-C(45)	1.421 (8)
Re-C(41)	2.266 (6)	C(41)-C(42)	1.435 (9)
Re-C(42)	2.216 (6)	C(42)-C(43)	1.412 (9)
Re-C(43)	2.244 (6)	C(43)-C(44)	1.396 (9)
Re-C(44)	2.258 (6)	C(44)-C(45)	1.381 (8)
Re-C(45)	2.235 (6)		
Bond Angles			
P(1)-Re-P(2)	95.92 (6)	P(2)-Re-H(41)	78 (2)
P(1)-Re-H(41)	88 (2)		

two phosphine ligands both point away from the five-membered ring of the indan ligand, creating a pseudo-mirror plane through middle of the indan molecule (bisecting C37-C38-C39). The benzene analog for this complex is also known.[10a,b,23]

Reaction of $ReH_7(PPh_3)_2$ with Indan. In an attempt to obtain **2** pure, $ReH_7(PPh_3)_2$ was also reacted with an excess of indan. Excess 3,3-dimethyl-1-butene was also added in order to facilitate the reaction with the aromatic substrate. Surprisingly, the major product of this reaction was **1** and not **2**. Apparently the energy required for the formation of **2** by direct attack at the aromatic ring is excessive (disruption of the aromaticity would result in a loss of up to 0.54β), while dehydrogenation of the saturated five-membered ring leading to the formation of **1** results in a concurrent gain in resonance stabilization energy of up to 1.58β.

Preparation of (η^4-C_9H_{12})$ReH_3(PPh_3)_2$ (7). In another early attempt to find a reaction in which **2** could be obtained pure, bicyclo[4.3.0]nona-3,6(1)-diene was reacted with $ReH_7(PPh_3)_2$. In previous studies with $Fe_2(CO)_9$, the 1,4-diene rearranged to a 1,3-diene, producing (η^4-bicyclo[4.3.0]nona-2,6(1)-diene)Fe-$(CO)_3$.[19] If reaction with $ReH_7(PPh_3)_2$ produced the analogous (η^4-bicyclo[4.3.0]nona-2,6(1)-diene)$ReH_3(PPh_3)_2$, this species should then be able to lose H_2 and form **2**. A sample of ReH_7-$(PPh_3)_2$ was therefore reacted with excess bicyclo[4.3.0]nona-3,6(1)-diene in THF, and the reaction was monitored by ^{1}H NMR spectroscopy. The single product that formed was not **2** (eq 4).

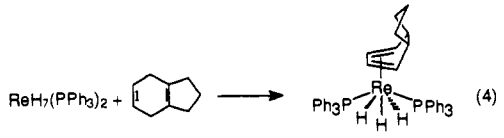

(4)

7

The ^{1}H NMR spectrum (Table I) indicated that the complex had a symmetrically bound (η^4-C_9H_{12}) ligand and that it was fluxional at room temperature (the spectrum showed a broad upfield peak which integrated as three equivalent hydrides and also showed equivalent phosphorus atoms). The bicyclo[4.3.0]nona-3,6(1)-diene had apparently rearranged to a 1,3-diene other than the one expected, namely, bicyclo[4.3.0]nona-2,4-diene.

This formulation was confirmed by single-crystal X-ray diffraction (Figure 7). Selected bond lengths and angles for **7** are listed in Table VI. The four carbon atoms that are bound to Re are planar to within 0.02 Å. There is disorder in the molecule at the apical methylene group C38. The disorder arises as to whether C38 points toward the diene fragment (molecule A, population = 57%) or away from the diene fragment (molecule B, population = 43%). The plane formed by C40, C41, C44, and C45 bends away from the Re atom at an angle of 42° from the diene plane, and the next plane of carbon atoms (C37, C39, C40, C45) bends an additional 57° away from the Re atom. The protons on the bridgehead carbons (H37 and H42) are cis and endo with respect to the Re atom. The structure shows that the phosphine atoms are actually inequivalent, as are the hydrides (one of the hydrides lies trans to the diene centroid, while the other two hydrides are equivalent). Since the ^{1}H NMR spectrum was fluxional at room temperature, a low-temperature ^{1}H NMR study was conducted in order to address the fluxional processes present.

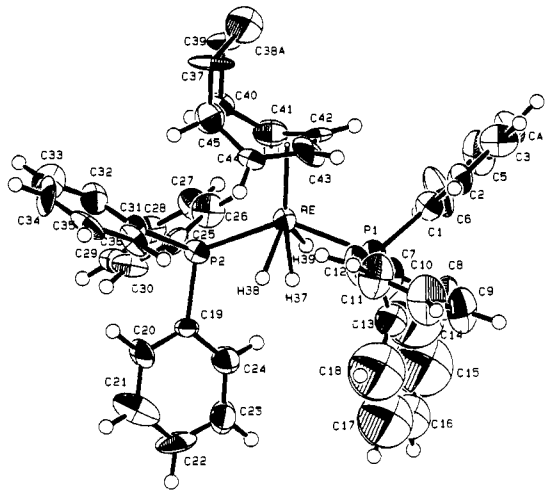

Figure 7. ORTEP diagram of **7a** with the thermal ellipsoids shown at 50% probability. The hydride ligands were located and refined.

Table VI. Selected Bond Distances (Å) and Angles (deg) for (η^4-C_9H_{12})$ReH_3(PPh_3)_2$ (7)

Bond Distances			
Re-P(1)	2.354 (5)	Re-H(37)	1.6 (1)
Re-P(2)	2.376 (5)	Re-H(38)	1.8 (1)
Re-C(41)	2.30 (2)	Re-H(39)	1.5 (1)
Re-C(42)	2.23 (2)	C(41)-C(42)	1.43 (3)
Re-C(43)	2.20 (2)	C(42)-C(43)	1.45 (3)
Re-C(44)	2.33 (2)	C(43)-C(44)	1.41 (3)
Bond Angles			
P(1)-Re-P(2)	139.9 (2)	P(2)-Re-H(38)	72 (4)
P(1)-Re-H(37)	74 (5)	P(2)-Re-H(39)	74 (5)
P(1)-Re-H(38)	83 (4)	H(37)-Re-H(38)	107 (6)
P(1)-Re-H(39)	66 (5)	H(37)-Re-H(39)	47 (6)
P(2)-Re-H(37)	83 (5)	H(38)-Re-H(39)	59 (6)

A sample of **7** in toluene-d_8 was cooled in the probe of the NMR spectrometer in order to obtain the static spectrum, and then the temperature was gradually raised and the ^{1}H NMR spectrum of **7** was monitored. The static spectrum of **7** obtained at −75 °C showed a spectrum that was consistent with the crystal structure. The hydrides were resolved as two separate resonances at δ −2.515 (t, J = 40.17 Hz, 1 H) and −7.253 (t, J = 18.0 Hz, 2 H). The ortho resonances of the phosphine ligands were also resolved at δ 8.129 and 7.654. When the temperature is raised, the first fluxional process that is seen is the equilibration of the phosphine ligands. This presumably takes place by the rotation of the diene ligand. At −42.5 °C, the ortho resonances coalesce. Using the temperature of coalescence and the peak separation from the static spectrum (190.3 Hz), the $\Delta G^{\ddagger}$ for this fluxional process is calculated to be 10.60 kcal/mol. The other fluxional process that is seen is the interconversion of the three hydride ligands. The hydride resonances coalesce at −5 °C, which corresponds to a $\Delta G^{\ddagger}$ of 11.18 kcal/mol ($\Delta\nu$ = 1896.3 Hz). These values are close to those reported for the related processes in the complex (η^4-C_5H_6)$ReH_3(PPh_3)_2$ of 12.1 and 12.3 kcal/mol, respectively.[10c] The high-temperature limit for the hydrides was reached at 60 °C. At this temperature, the hydride resonance appears at δ −5.844 (t, J = 26.4 Hz, 3 H).

Thermal Chemistry of 7: Preparation of (η^5-C_9H_{11})ReH_2-$(PPh_3)_2$ (8). A sample of **7** in C_6D_6 was heated to 90 °C, and the reaction was monitored by ^{1}H NMR spectroscopy. The hydride resonance of **7** was seen to broaden at this temperature, and two products were seen to grow in (eq 5). One of the products

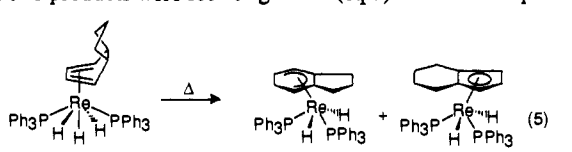

(5)

7 2 8

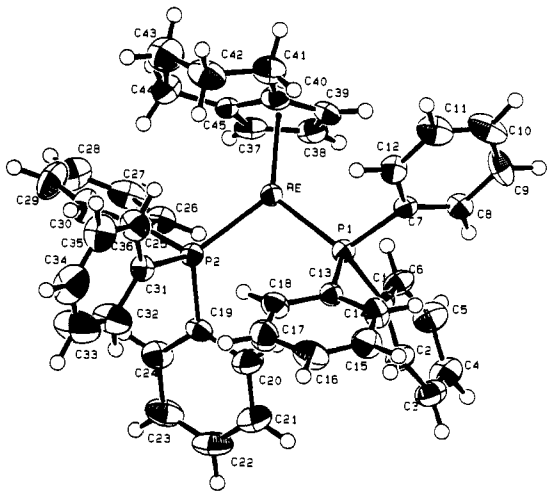

Figure 8. ORTEP diagram of **8** with the thermal ellipsoids shown at 50% probability. The hydride ligands were not located.

Table VII. Selected Bond Distances (Å) and Angles (deg) for $(\eta^5\text{-}C_9H_{11})ReH_2(PPh_3)_2$ (**8**)

Bond Distances			
Re–P(1)	2.328 (2)	Re–C(45)	2.281 (7)
Re–P(2)	2.322 (2)	C(37)–C(38)	1.42 (1)
Re–C(37)	2.220 (7)	C(37)–C(45)	1.43 (1)
Re–C(38)	2.245 (8)	C(38)–C(39)	1.41 (1)
Re–C(39)	2.306 (8)	C(39)–C(40)	1.40 (1)
Re–C(40)	2.335 (8)	C(40)–C(45)	1.45 (1)
Bond Angle			
P(1)–Re–P(2)	105.95 (7)		

was **2**, but it was the minor product. The other product was apparently η^5-bound to the five-membered ring since there were resonances in the region of metal-bound Cp ligands similar to those of **1**. The remaining resonances were between δ 2.2 and 1.2, indicating that the six-membered ring was saturated and that the diene of **7** had rearranged to a 4,5,6,7-tetrahydroindenyl ligand. The triplet hydride resonance, integrating as two hydrides, indicated two equivalent phosphorus atoms (Table I). This data allowed the formulation of the complex as $(\eta^5\text{-}C_9H_{11})ReH_2(PPh_3)_2$ (**8**). This formulation was confirmed by single-crystal X-ray diffraction (Figure 8). Selected bond lengths and angles for **8** are listed in Table VII. The five carbons that are bound to Re are planar to within 0.003 Å. The structure is very similar to that reported for $CpReH_2(PPh_3)_2$.[10c]

The mechanism for the formation of **8** is unclear. Formally, all nine carbons of the diene ligand in **7** are involved in the mechanism. The four carbons that are bound to the Re atom in **7** are hydrogenated and the remaining five carbon atoms are dehydrogenated. The protons on the bridgehead carbons H37 and H42 lie 3.62 and 3.51 Å away from the Re, respectively, and are only slightly further than the methylene endo proton in **2** (3.26 Å). Therefore, it is reasonable to assume that, upon heating, **7** loses H_2 and that this is then followed by the migration of one of the bridgehead protons to the Re atom. The metal hydride can now migrate back to the ring, returning either to the bridgehead position or to the 5 position. Several such hydride migrations could lead to the formation of both **2** and **8**. Alternatively, a mechanism in which there is cleavage of the C–C bridgehead bond followed by the formation of a new bridgehead bond (with several hydride migrations also occurring) cannot be ruled out, but seems implausible since such ring transformations have not been seen before in these systems.

Oxidation/Protonation of 2: Preparation of $[(\eta^6\text{-}C_9H_{10})ReH_2(PPh_3)_2][X]$ (X = ReO_4, 9; BF_4, 10). In an earlier attempt to separate complexes **1** and **2**, a mixture of **1** and **2** was reacted with $[Cp_2Fe][BF_4]$. It has been previously shown that $CpReH_2(PPh_3)_2$ can be reversibly oxidized by one electron,[25] and

(25) Detty, M. R.; Jones, W. D. *J. Am. Chem. Soc.* **1987**, *109*, 5666.

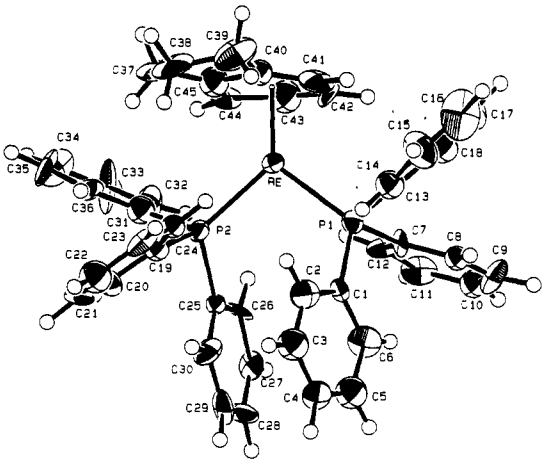

Figure 9. ORTEP diagram of **9** with the thermal ellipsoids shown at 50% probability. The hydride ligands were not located.

Table VIII. Selected Bond Distances (Å) and Angles (deg) for $[(\eta^6\text{-}C_9H_{10})Re(PPh_3)_2H_2]^+[ReO_4]^-$ (**9**)

Bond Distances			
Re–P(1)	2.382 (7)	Re–C(45)	2.32 (3)
Re–P(2)	2.360 (6)	C(40)–C(41)	1.40 (3)
Re–C(40)	2.33 (3)	C(40)–C(45)	1.44 (3)
Re–C(41)	2.22 (2)	C(41)–C(42)	1.40 (3)
Re–C(42)	2.25 (2)	C(42)–C(43)	1.35 (3)
Re–C(43)	2.30 (2)	C(43)–C(44)	1.42 (3)
Re–C(44)	2.27 (2)	C(44)–C(45)	1.45 (3)
Bond Angle			
P(1)–Re–P(2)	100.0 (2)		

Scheme II. Reactions of $ReH_7(PPh_3)_2$

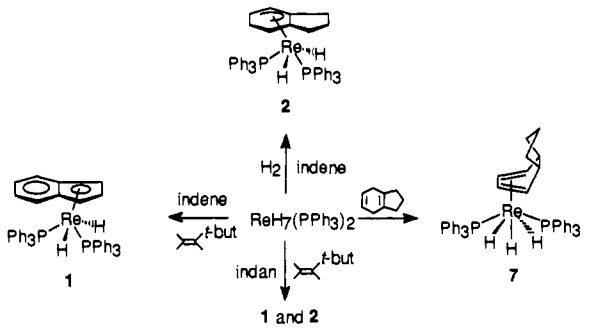

we had hoped to selectively oxidize **1**, which would allow the facile separation of the two complexes. Unfortunately, it was **2** that was selectively oxidized by $[Cp_2Fe][BF_4]$ (the ^1H NMR resonances for **2** disappear, while those of **1** remain unchanged), and the subsequent electron-transfer catalysis that takes place (presumably with a similar mechanism as for $CpReH_2(PPh_3)_2$)[25] results in the quantitative formation of $[(\eta^6\text{-}C_9H_{10})ReH_2(PPh_3)_2][BF_4]$ (**10**) as evidenced by its ^1H NMR spectrum, which indicated the presence of an η^6-indan ligand, two equivalent metal hydrides, and two equivalent phosphine ligands.

Exchange of the BF_4 anion of **10** with ReO_4 by stirring **10** with excess $KReO_4$ in $CHBr_3$ resulted in the formation of the analogous $[(\eta^6\text{-}C_9H_{10})ReH_2(PPh_3)_2][ReO_4]$ (**9**). This formulation was confirmed by single-crystal X-ray diffraction (Figure 9). Selected bond lengths and angles for **9** are listed in Table VIII. The six carbon atoms that are bound to Re are planar to within 0.04 Å.

Conclusions. The reactions conducted herein of $ReH_7(PPh_3)_2$ with various indene-related substrates are summarized in Scheme II. We have shown that the reaction of indene with $ReH_7(PPh_3)_2$ produces organometallic complexes in which the metal is bound on either the five- or six-membered ring. The ratio of these products can be altered in a rational fashion by varying the reaction conditions used.

We have found that metal hydride to ring migrations are very prevalent throughout this and other reactions reported herein and that these migrations are facile and are often accompanied by facile metal–carbon migrations, resulting in the metal "walking" across from the five-membered ring to the six-membered ring (the reverse is also seen). We have also been able to obtain the activation parameters for several fluxional processes, including both ring rotation and metal hydride interconversions.

Experimental Section

General Procedures. Nearly all of the compounds that were used in this work are only slightly air sensitive in the solid state, but are unstable in solution toward prolonged exposure to oxygen and moisture. All reactions were performed under vacuum or a nitrogen atmosphere in a Vacuum Atmospheres Dry-Lab glovebox. All reagents were obtained commercially and put through three freeze–pump–thaw cycles for degassing before use. All deuterated solvents were purchased from MSD Isotopes Merck Chemical Division, distilled under vacuum from dark purple solutions of benzophenone ketyl, and stored in ampules with Teflon-sealed vacuum line adapters. All other solvents were dried similarly and stored in the glovebox.

Proton, carbon, and phosphorus NMR spectra were recorded on a Bruker AMX-400 NMR spectrometer. ^{1}H NMR chemical shifts were measured in ppm (δ) relative to tetramethylsilane, using the residual ^{1}H resonances in the deuterated solvents as an internal reference: C_6D_6 (δ 7.15), toluene-d_8 (δ 2.09), and THF-d_8 (δ 3.58). ^{13}C NMR chemical shifts were measured in ppm relative to C_6D_6 (δ 128). ^{31}P NMR chemical shifts were measured relative to 30% H_3PO_4. Elemental analyses were carried out at Desert Analytics-Organic Microanalysis Laboratory. An Enraf-Nonius CAD4 diffractometer was used for X-ray crystal structure determination. Photolyses were carried out by using a high-pressure 200-W Hg focused-beam Oriel lamp fitted with an infrared-absorbing water filter. Experiments involving more than one sample to be photolyzed under identical conditions were carried out in a merry-go-round apparatus. GC–MS spectra were taken using a Hewlett-Packard 5890 Series II gas chromatograph.

The synthesis of $ReH_7(PPh_3)_2$ was as previously reported.[10c] The synthesis of $ReD_7(PPh_3)_2$ was the same as for $ReH_7(PPh_3)_2$, but LAD and D_2O were used in place of LAH and H_2O.

Reaction of $ReH_7(PPh_3)_2$ with Indene. To a stirred solution of 200 mg (0.27 mmol) of $ReH_7(PPh_3)_2$ in 20 mL of THF was added 0.65 mL (5.57 mmol) of indene. The reaction was stirred overnight, resulting in a yellow-brown solution. The solvent was evaporated in vacuo and the crude yellow-brown solid was dried overnight. A ^{1}H NMR spectrum of the solid revealed a 1:2 mixture of complexes **1** and **2**. The complexes could be purified by recrystallization from diethyl ether, but could not be separated by chromatographic methods or selective recrystallization. Alternative reactions were employed in order to obtain each compound pure.

Reaction of $ReD_7(PPh_3)_2$ with Indene. Conditions identical to those used in the above reaction were used with $ReD_7(PPh_3)_2$ in place of $ReH_7(PPh_3)_2$. A ^{1}H NMR spectrum of the resulting solid again revealed a 1:2 mixture of complexes **1** and **2**. Integration of the ^{1}H NMR resonances of **2** revealed which positions of the indanyl ligand had been deuterated and to what extent they were deuterated.

Reaction of $ReH_7(PPh_3)_2$ with Indan. To a stirred solution of 200 mg (0.27 mmol) of $ReH_7(PPh_3)_2$ in 20 mL of THF was added 1 mL (8.36 mmol) of 3,3-dimethyl-1-butene followed by 1.0 mL (8.17 mmol) of indan. The reaction was stirred overnight, resulting in a brown solution. The solvent was evaporated in vacuo to give a brownish-yellow solid. ^{1}H NMR spectroscopy showed the formation of **1** and **2** in a ratio of **1**:**2** = 5.

Preparation of (η^5-C_9H_7)$ReH_2(PPh_3)_2$ (1). To a stirred solution of 200 mg (0.27 mmol) of $ReH_7(PPh_3)_2$ in 20 mL of THF was added 1 mL (8.36 mmol) of 3,3-dimethyl-1-butene followed by 0.65 mL (5.57 mmol) of indene. The reaction was stirred overnight and resulted in an orange-brown solution. The solvent was evaporated in vacuo to give an orange solid. The crude product was dissolved in 5 mL of diethyl ether and allowed to stand overnight to give 180 mg (78%) of **1** as yellow crystals. Anal. Calcd for $C_{45}H_{39}P_2Re$: C, 65.28; H, 4.75. Found: C, 65.03; H, 4.89.

Observation of (η^4-C_9H_{10})$ReH_3(PPh_3)_2$ (3). A sample of 10 mg of $ReH_7(PPh_3)_2$ in 0.45 mL of C_6D_6 was placed in a resealable NMR tube. The sample was then placed under an atmosphere of H_2 and the reaction was monitored by ^{1}H NMR spectroscopy. In addition to the resonances of **2**, there were also several other resonances observed. The unbound olefinic protons and the hydrides (high-temperature limit) of **3** were easy to assign due to their chemical shifts and their coupling patterns. The remaining two protons on the six-membered ring were found through ^{1}H–^{1}H homonuclear decoupling. The six protons on the saturated five-membered ring were too obscured by the resonances of **2** (as were those of the phosphine ligands) to assign. ^{1}H NMR (C_6D_6): δ 5.158 (d, J = 4.8 Hz, 1 H, H^1), 4.705 (dd, J = 4.8, 6.0 Hz, 1 H, H^2), 2.546 (t, J = 5.8 Hz, 1 H, H^3), 1.602 (d, J = 5.7 Hz, 1 H, H^4), −7.67 (t, J = 41.1 Hz, 3 H).

Preparation of (η^5-C_9H_{11})$ReH_2(PPh_3)_2$ (2). To a stirred solution of 150 mg (0.21 mmol) of $ReH_7(PPh_3)_2$ in 20 mL of THF was added 0.65 mL (5.57 mmol) of indene. The sample was then placed under an atmosphere of H_2 and the reaction was stirred overnight, resulting in a yellow-brown solution. The solvent was evaporated in vacuo to give a brownish solid. The crude product was dissolved in 5 mL of diethyl ether and allowed to stand overnight to give 150 mg (86%) of **2** as yellow crystals. Anal. Calcd for $C_{45}H_{43}P_2Re$: C, 64.96; H, 5.21. Found: C, 65.02; H, 5.28.

Kinetics of the Reaction of $ReH_7(PPh_3)_2$ and Indene. For the indene concentration study, a 0.034 M solution of $ReH_7(PPh_3)_2$ in 1.5 mL of C_6D_6 was made, and 10 μL of n-pentane was then added as an internal standard. This solution was separated into three 0.45-mL portions, and aliquots of indene (5, 15, and 50 μL) were added to each sample. The reaction was then monitored by ^{1}H NMR spectroscopy. For the $ReH_7(PPh_3)_2$ concentration study, two samples were prepared with different $ReH_7(PPh_3)_2$ concentrations (0.038 and 0.005 M) in C_6D_6. To each sample was added 10 μL of n-pentane and 15 μL of indene. The reaction was then monitored by ^{1}H NMR spectroscopy.

Photolysis of 1. Two samples of 5 mg of **1** in 0.45 mL of C_6D_6 were placed in resealable NMR tubes. To the first sample was added 0.73 mmol of PMe_3 (50 equiv, 50 mmHg, 273 mL, 22 °C). To the second sample was condensed in 0.73 mmol of n-pentane (50 equiv, 50 mmHg, 273 mL, 22 °C). Each sample was then irradiated for 48 h with and without a $\lambda > 345$ nm filter, and the reactions were monitored by ^{1}H NMR spectroscopy. No changes were seen in the spectra for any of the reactions.

Thermolysis of 1. Three identical samples were prepared of 5 mg of **1** in 0.45 mL of toluene-d_8. To each of these samples was added 0.05 mL of PMe_3. The three samples were then heated at 50, 100, and 150 °C in oil baths. The reactions were monitored by ^{1}H NMR spectroscopy. The only sample that showed any reaction was the one at 150 °C. For this sample, new hydride resonances were seen to grow in at δ −8.77 (qt of d, J = 23.2, 13.0 Hz), −11.15 (dd, J = 41.4, 45.2 Hz), and −11.926 (t, J = 43.8 Hz) corresponding to $HRe(PMe_3)_5$, (η^5-C_9H_7)ReH_2-$(PPh_3)(PMe_3)$, and (η^5-C_9H_7)$ReH_2(PMe_3)_2$, respectively.

Variable-Temperature Equilibrium Ratios of 2:3. An NMR sample of 10 mg (0.01 mmol) of **2** in 0.45 mL of toluene-d_8 was heated to various temperatures in the probe of the NMR spectrometer, and the ratio of **2**:**3** was monitored by integration of the hydride resonances at δ −7.67 (**3**) and −11.26 (**2**).

Preparation of (η^6-C_9H_{10})$ReH_3(PPh_3)$ (5). An NMR sample of 10 mg (0.01 mmol) of **2** in 0.45 mL of C_6D_6 was irradiated with a $\lambda > 345$ nm filter for 24 h. The reaction was followed by ^{1}H NMR spectroscopy showing the quantitative conversion of **2** to **5** and the formation of free triphenylphosphine. The solvent was removed in vacuo, and the crude product was then dissolved in 1 mL of diethyl ether. Upon the solution standing overnight, several crystals were obtained and a crystal structure analysis of **5** was undertaken. The reaction was also run with 280 mg (0.34 mmol) of **2** in 10 mL of THF, giving 180 mg (93.9%) of **5** as a bright yellow powder after washing with 5 mL of diethyl ether. Anal. Calcd for $C_{45}H_{41}P_2Re$: C, 56.92; H, 4.95. Found: C, 56.21; H, 4.95.

Preparation of (η^6-C_9H_{10})$ReH(PPh_3)_2$ (6). An NMR sample of 10 mg (0.01 mmol) of **2** in 0.45 mL of C_6D_6 was heated to 90 °C for 24 h. The reaction was followed by ^{1}H NMR spectroscopy, and it showed the quantitative conversion of **2** to **6** and the formation of free H_2. The solvent was removed in vacuo, and the crude product was then dissolved in 1 mL of diethyl ether. Upon the solution standing overnight, several crystals were obtained and a crystal structure analysis of **6** was undertaken. The reaction was also run with 280 mg (0.34 mmol) of **2** in 10 mL of benzene, giving 255 mg (91.3%) of **6**.

Preparation of (η^4-C_9H_{12})$ReH_3(PPh_3)_2$ (7). To a stirred solution of 80 mg (0.11 mmol) of $ReH_7(PPh_3)_2$ in 20 mL of THF was added 0.25 mL (2.09 mmol) of 3,3-dimethyl-1-butene followed by 0.5 mL of bicyclo[4.3.0]nona-3,6(1)-diene (3.87 mmol). The reaction was stirred overnight and resulted in a yellow-brown solution. The solvent was evaporated in vacuo to give a brownish solid. The crude product was dissolved in 5 mL of diethyl ether and allowed to stand overnight to give 78 mg (85%) of **7** as colorless crystals. Anal. Calcd for $C_{45}H_{45}P_2Re$: C, 64.81; H, 5.44. Found: C, 64.77; H, 5.55.

Preparation of (η^5-C_9H_{11})$ReH_2(PPh_3)_2$ (8). A stirred solution of 25 mg (0.03 mmol) of **7** in 5 mL of toluene was heated at 60 °C for 2 h. The solvent was removed in vacuo to give a brownish solid. A ^{1}H NMR spectrum of the solid revealed a 1:1.5 mixture of **2** and **8**. The crude

Table IX. Summary of Crystallographic Data for **1**, **2**, and **5–9**

	1	**2**	**5**	**6**	**7**	**8**	**9**
empirical formula	$C_{45}H_{39}P_2Re$	$C_{45}H_{43}P_2Re$	$C_{27}H_{28}PRe$	$C_{45}H_{41}P_2Re$	$C_{45}H_{45}P_2Re$	$C_{45}H_{43}P_2Re$	$[C_{45}H_{42}P_2Re][ReO_4]$
cryst syst	triclinic	triclinic	triclinic	monoclinic	monoclinic	triclinic	monoclinic
space group	$P\bar{1}$ (No. 2)	$P\bar{1}$	$P\bar{1}$	$P2_1/n$ (No. 14)	$P2_1/n$	$P\bar{1}$	$P2_1/n$
Z	2	2	2	4	4	2	4
a, Å	9.876 (7)	10.140 (4)	8.626 (3)	10.428 (3)	14.418 (2)	10.104 (3)	11.950 (3)
b, Å	14.137 (4)	13.993 (5)	9.201 (2)	17.054 (3)	16.823 (4)	14.344 (5)	18.836 (8)
c, Å	14.375 (12)	14.564 (9)	16.002 (5)	20.100 (4)	15.838 (7)	14.475 (5)	17.781 (5)
α, deg	96.12 (6)	95.51 (4)	97.43 (2)	90	90	71.85 (3)	90
β, deg	109.07 (6)	109.73 (4)	98.34 (3)	98.78 (2)	102.72 (2)	69.42 (2)	98.28 (2)
γ, deg	107.99 (5)	107.58 (3)	114.12 (3)	90	90	71.01 (3)	90
V, Å^3	1755 (5)	1809 (4)	1122 (1)	3532 (2)	3747 (3)	1811 (2)	3961 (4)
d_{calcd}, g/cm^3	1.566	1.528	1.732	1.560	1.478	1.526	1.395
T, °C	−75	25	25	0	25	0	25
diffractometer	Enraf-Nonius CAD4	Enraf-Nonius CAD4	Enraf-Nonius CAD4	Enraf-Nonius CAD4	Enraf-Nonius CAD4	Enraf-Nonius CAD4	Enraf-Nonius CAD4
$\lambda_{Mo K\alpha}$ (graphite monochromated radiation)	0.71069	0.71069	0.71069	0.71069	0.71069	0.71069	0.71069
scan type	$2\theta/\omega$	$2\theta/\omega$	$2\theta/\omega$	$2\theta/\omega$	$2\theta/\omega$	$2\theta/\omega$	$2\theta/\omega$
scan rate, deg/min	2–16.5	2–16.5	2–16.5	2–16.5	2–16.5	2–16.5	2–16.5
total background time	scan time/2	scan time/2	scan time/2	scan time/2	scan time/2	scan time/2	scan time/2
take-off angle, deg	2.6	2.6	2.6	2.6	2.6	2.6	2.6
scan range, deg	0.8 + 0.35 tan θ	0.8 + 0.35 tan θ	0.8 + 0.35 tan θ	0.8 + 0.35 tan θ	0.8 + 0.35 tan θ	0.8 + 0.35 tan θ	0.8 + 0.35 tan θ
2θ range, deg	2–22	2–21	2–25	2–22	2–22	2–22	2–21
data collected	$+h,\pm k,\pm l$	$+h,\pm k,\pm l$	$+h,\pm k,\pm l$	$+h,+k,\pm l$	$+h,+k,\pm l$	$+h,\pm k,\pm l$	$+h,+k,\pm l$
no. of data collected	4595	5349	4212	4780	4396	4734	4653
no. of unique data > 3σ	3696	1918	1906	3199	2140	3739	2070
no. of params varied	441	388	274	437	396	433	408
abs coeff, cm^{-1}	36.28	35.21	55.72	36.06	33.99	35.18	32.16
systematic absences	none	none	none	$0k0$, k odd $h0l$, $h+l$ odd	$0k0$, k odd $h0l$, $h+l$ odd	none	$0k0$, k odd $h0l$, $h+l$ odd
abs correction	differential	differential	differential	differential	differential	differential	differential
range of transm factors	0.83–1.25	0.72–1.18	0.76–1.14	0.93–1.09	0.85–1.24	0.86–1.14	0.86–1.12
equiv data	$0kl$, $0\bar{k}\bar{l}$	$0kl$, $0\bar{k}\bar{l}$	$0kl$, $0\bar{k}\bar{l}$	$0kl$, $0k\bar{l}$	$0kl$, $0k\bar{l}$	$0kl$, $0\bar{k}\bar{l}$	$0kl$, $0k\bar{l}$
agreement of equiv data (F_o)	0.023	0.175	0.086	0.029	0.067	0.031	0.086
R_1	0.033	0.062	0.045	0.024	0.048	0.034	0.046
R_2	0.049	0.056	0.040	0.027	0.048	0.039	0.043
goodness of fit	2.02	1.16	1.01	1.02	1.37	1.46	1.15
largest peak in final E map	1.04	0.90	0.66	0.38	1.20	0.53	0.80

product was dissolved in 5 mL of diethyl ether, giving 22 mg of a dark yellow solid after filtration (88% combined yield). Recrystallization from diethyl ether gave **8** as large brownish yellow plates. The plates were then dissolved in diethyl ether and allowed to stand overnight, giving yellow X-ray quality crystals of **8**.

Preparation of $[(\eta^6\text{-}C_9H_{10})ReH_2(PPh_3)_2][ReO_4]$ (9). To a stirred solution of 25 mg (0.027 mmol) of **10** in 5 mL of $CHBr_3$ was added 79 mg (0.25 mmol) of $KReO_4$. The reaction was stirred overnight with no apparent color change. The solvent was removed in vacuo, and the product was extracted with 5 mL of benzene. Slow evaporation of the solvent gave pale yellow crystals, and a structural analysis of **9** was undertaken.

Preparation of $[(\eta^6\text{-}C_9H_{10})ReH_2(PPh_3)_2][BF_4]$ (10). To a stirred solution of 100 mg (0.12 mmol) of **2** in 5 mL of THF was added 34 mg (0.13 mmol) of $[Cp_2Fe][BF_4]$. The reaction was stirred overnight, resulting in an orange-yellow solution. The solvent was removed in vacuo, and the resulting solid was washed with 5 mL of diethyl ether, giving an off-white solid and an orange solution (Cp_2Fe). Filtration of the solution gave 90 mg (81%) of **10** as a white solid. Anal. Calcd for $C_{45}H_{42}BF_4P_2Re$: C, 58.89; H, 4.61. Found: C, 58.02; H, 4.56.

Solution and Refinement of Crystal Structures. $(\eta^5\text{-}C_9H_7)ReH_2(PPh_3)_2$ (1). A yellow crystal of **1** with approximate dimensions 0.2 × 0.25 × 0.1 mm^3 was mounted on a glass fiber and placed on the diffractometer under a stream of nitrogen at −75 °C. The lattice constants were obtained from 25 centered reflections with values of χ between 10 and 60°. Cell reduction revealed a primitive triclinic crystal system. Data were collected in accord with the parameters in Table IX. The intensities of three representative reflections which were measured after every 60 min of X-ray exposure time remained constant throughout data collection, indicating crystal stability. The space group was assigned as $P\bar{1}$, and the correctness of this choice was confirmed by the successful solution of the Patterson map, showing the Re atom. The structure was expanded by using the DIRDIF program supplied by the Molecular Structure Corp., whose programs were used for further refinement of the structure. An empirical absorption correction was applied after isotropic refinement of all non-hydrogen atoms by using the program DIFABS. Anisotropic refinement of all non-hydrogen atoms was carried out with hydrogen atoms attached to carbons in fixed, idealized positions (thermal parameters set to 1.2 × B_{iso}(carbon)). A difference Fourier map was then calculated using only data with sin $\theta/\lambda < 0.34$ ($\theta < 14°$). The largest two peaks (0.5 e/Å^3) were in positions corresponding to the expected locations for the two hydride ligands on the basis of the geometry of the other ligands. (The next largest peaks, nos. 3–5, were 0.3 e/Å^3 and were not within bonding distance to any atom in the molecule). Final refinement included these peaks as "hydride" ligands in which their positional and thermal parameters were refined. Selected bond distances and angles are given in Table II.

$(\eta^5\text{-}C_9H_{11})ReH_2(PPh_3)_2$ (2). A yellow crystal of **2** with approximate dimensions 0.25 × 0.1 × 0.2 mm^3 was mounted on a glass fiber and placed on the diffractometer at 25 °C. Data collection and reduction were as for **1** with a primitive triclinic crystal system, in accord with the parameters in Table IX. The space group was assigned as $P\bar{1}$. The crystal diffracted weakly, as only 1918 out of 5012 data were judged observed. Anisotropic refinement of all non-hydrogen atoms was carried out with hydrogen atoms attached to carbons in fixed, idealized positions (thermal parameters set to 1.2 × B_{iso}(carbon)). The hydrogens attached to the Re atom were not located. Selected bond distances and angles are given in Table III.

$(\eta^6\text{-}C_9H_{10})ReH_3(PPh_3)$ (5). A yellow crystal of **5** with approximate dimensions 0.15 × 0.1 × 0.1 mm^3 was mounted on a glass fiber and placed on the diffractometer under a stream of nitrogen at 0 °C. Data collection and reduction were as for **1** with a primitive triclinic crystal system, in accord with the parameters in Table IX. The space group was assigned as $P\bar{1}$. Anisotropic refinement of all non-hydrogen atoms was carried out with hydrogen atoms attached to carbon included in fixed, idealized positions (thermal parameters set to 1.2 × B_{iso}(carbon)). A difference Fourier map was now calculated using only data with sin $\theta/\lambda < 0.34$ ($\theta < 14°$). The three largest peaks (0.4 e/Å^3) were in positions corresponding to those expected for the three hydride ligands on the basis of the geometry of the other ligands. (The next largest peaks, nos. 4 and

5, were 0.2 e/Å^3 and were not within bonding distance to any atom in the molecule). Final refinement included these peaks as "hydride" ligands in which their positional and thermal parameters were refined. Selected bond distances and angles are given in Table IV.

(η^5-C_9H_{10})ReH(PPh_3)$_2$ (6). A yellow crystal of **6** with approximate dimensions 0.1 × 0.3 × 0.2 mm^3 was mounted on a glass fiber and placed on the diffractometer at 25 °C. Data collection and reduction were as for **1** with a monoclinic crystal system, in accord with the parameters in Table IX. The space group was uniquely assigned as $P2_1/n$. Anisotropic refinement of all non-hydrogen atoms was carried out with hydrogen atoms attached to carbon included in fixed, idealized positions (thermal parameters set to 1.2 × B_{iso}(carbon)). A difference Fourier map was now calculated using only data with sin $\theta/\lambda < 0.34$ ($\theta < 14°$). The largest peak (0.5 e/Å^3) was in a position corresponding to that expected for the hydride ligand on the basis of the geometry of the other ligands. (The next largest peaks, nos. 2-5, were 0.1-0.2 e/Å^3 and were not within bonding distance to any atom in the molecule.) Final refinement included this peak as a "hydride" ligand in which the positional and thermal parameters were refined. Selected bond distances and angles are given in Table V.

(η^4-C_9H_{12})ReH$_3$(PPh_3)$_2$ (7). A yellow crystal of **7** with approximate dimensions 0.15 × 0.25 × 0.15 mm^3 was mounted on a glass fiber and placed on the diffractometer at 25 °C. Data collection and structure refinement were as for **1** with a monoclinic crystal system. Data were collected in accord with the parameters in Table IX. The space group was uniquely assigned as $P2_1/n$. The isotropically refined model showed evidence for disorder of C38 between two possible locations, and consequently a second carbon (C38B) was introduced and refined isotropically, allowing the populations of C38A and C38B to vary together. One of the phenyl groups was also refined as a rigid group with isotropic thermal parameters as anisotropic refinement led to nonpositive definite values. Anisotropic refinement of all remaining non-hydrogen atoms was carried out with hydrogen atoms attached to carbons in fixed, idealized positions (thermal parameters set to 1.2 × B_{iso}(carbon); disordered hydrogens omitted on atoms C37-C39). A difference Fourier map was then calculated using only data with sin $\theta/\lambda < 0.34$ ($\theta < 14°$). Three peaks among the top eight peaks (0.4-0.6 e/Å^3) were in locations corresponding to the expected locations for the three hydride ligands on the basis of the geometry of the other ligands. (The other largest peaks, nos. 1, 2, and 5-7, were all in between the carbon atoms of the rigid phenyl group.) Final refinement included these peaks as "hydride" ligands in which their positional and thermal parameters were refined. The isotropic thermal parameter for the central hydride went slightly negative and was consequently fixed at 1.0. Selected bond distances and angles are given in Table VI.

(η^5-C_9H_{11})ReH$_2$(PPh_3)$_2$ (8). A yellow crystal of **8** with approximate dimensions 0.15 × 0.2 × 0.25 mm^3 was mounted on a glass fiber and placed on the diffractometer under a stream of nitrogen at 0 °C. Data collection and structure refinement were as for **1** with a primitive triclinic crystal system. Data were collected in accord with the parameters in Table IX. The space group was assigned as $P\bar{1}$. The hydrogens attached to the Re atom were not located. Selected bond distances and angles are given in Table VII.

[(η^6-C_9H_{10})ReH$_2$(PPh_3)$_2$][ReO$_4$] (9). A yellow crystal of **9** with approximate dimensions 0.2 × 0.1 × 0.2 mm^3 was mounted on a glass fiber and placed on the diffractometer at 25 °C. Data collection and structure refinement were as for **1** with a monoclinic crystal system, in accord with the parameters in Table IX. The space group was uniquely assigned as $P2_1/n$. The hydrogens attached to the Re atom were not located. Selected bond distances and angles are given in Table VIII.

Acknowledgement is made to the U.S. Department of Energy (Grant FG02-86ER-13569) and to NATO for a travel grant.

Supplementary Material Available: Tables of fractional atomic coordinates, bond distances and angles, and thermal parameters (80 pages); tables of calculated and observed structure factors (129 pages). Ordering information is given on any current masthead page.

Equilibrium Acidities of Some Transition-Metal Acyl Compounds

Maria C. Fermin, B. Thiyagarajan, and Joseph W. Bruno*

Contribution from the Hall-Atwater Laboratories, Wesleyan University, Middletown, Connecticut 06459. *Received July 27, 1992*

Abstract: There is readily available a series of stable niobium acyl and iminoacyl compounds of the general formula [(η^5-$C_5H_4SiMe_3$)$_2$Nb(X)(η^2-CECHR$_2$)][BF_4] (E = O, NR; X = H, Cl); these are prepared by protonation of their conjugate bases, the corresponding ketene, or ketene imine complexes. These proton-transfer equilibria have been studied in dimethyl sulfoxide or acetonitrile with organic acids of known pK_a, allowing for the determination of enolization pK_as for the η^2-acyl and -iminoacyl ligands. The acyls are appreciably more acidic than are the corresponding phenyl ketones (those in which a phenyl group replaces niobium), with pK_a differences of ca. 18-24 pK units. The acyls are somewhat less sensitive to changes in substituents at the ionizing position than are the ketones, but they are surprisingly sensitive to the electronic properties of the neighboring ligand. A few representative η^1-acyl compounds have been studied, and these are substantially less acidic than are the organic ketones. The enhanced acidity of the η^2-acyls is thus attributed to the interaction of the cationic niobium center with the acyl heteroatom, and the data contribute to a semiquantitative understanding of the influence of the metal on the solution chemistry of the acyl ligand.

Introduction

The η^2-acyl ligand was first identified in 1971,[1] and it has been the subject of extensive study ever since.[2] The interest in this ligand stems primarily from its role in the reduction of carbon monoxide, a process that has been shown to involve many reactions that are unavailable to η^1-acyls.[3] Since these include a variety of insertion, C-C coupling, and hydrogen migration reactions, η^2-acyls were originally considered to possess a substantial oxycarbene character. However, recent theoretical studies have

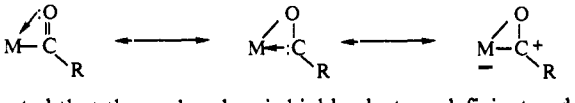

indicated that the acyl carbon is highly electron-deficient and is therefore better described as a carbenium ion center.[4] The

(1) Hitch, R. R.; Gondal, S. K.; Sears, C. T. *Chem. Commun.* **1971**, 777-778.
(2) Durfee, L. D.; Rothwell, I. P. *Chem. Rev.* **1988**, *88*, 1059-1079.
(3) (a) Cummins, C. C.; Van Duyne, G. D.; Schaller, C. P.; Wolczanski, P. T. *Organometallic* **1991**, *10*, 164-170. (b) Roddick, D. M.; Bercaw, J. E. *Chem. Ber.* **1989**, *122*, 1579-1587.
(4) Tatsumi, K.; Nakamura, A.; Hofmann, P.; Stauffert, P.; Hoffmann, R. *J. Am. Chem. Soc.* **1985**, *107*, 4440-4451.

0002-7863/93/1515-974$04.00/0